Monthly Notices
of the
ROYAL ASTRONOMICAL SOCIETY

MNRAS **433,** 2893–2899 (2013)
Advance Access publication 2013 June 27

doi:10.1093/mnras/stt910

On the (non-)universality of the mixing length parameter

F. J. G. Pinheiro[1,2]⋆ and J. Fernandes[1,2,3]

[1]*Centro de Geofísica da Universidade de Coimbra, Av. Dr. Dias da Silva, P-3000-134 Coimbra, Portugal*
[2]*Observatório Astronómico da Universidade de Coimbra, Santa Clara, P-3040-004 Coimbra, Portugal*
[3]*Departamento de Matemática da Universidade de Coimbra, Largo D. Dinis, P-3001-454 Coimbra, Portugal*

Accepted 2013 May 22. Received 2013 May 21; in original form 2012 October 4

ABSTRACT

The success of the Böhm-Vitense formalism – the so-called mixing length theory – for the treatment of the energy transport in the superadiabatic stellar region in reproducing the properties of the Sun and other stars is well testified by the fact that it is commonly used in almost all stellar evolutionary codes. Yet, several results are pointing out against such an assumption. In this work, we address the universality of the mixing length parameter and search for a possible dependence on several global stellar parameters. While we observe a significant degree of correlation between the mixing length parameter and both the stellar mass and effective temperature. No such indication is found regarding the stellar activity, as stated by previous works.

Key words: stars: evolution – stars: fundamental parameters – stars: interiors.

1 INTRODUCTION

Stellar evolutionary models are fundamental for different areas of astronomy, such as the determination of stellar masses and ages from an HRD analysis (i.e. the use of their position in the H-R diagram). The computation of stellar models generally involves the use of parameters, such as Böhm-Vitense's (1958) mixing length, in order to describe physical mechanisms which are insufficiently known (e.g. Cassisi 2005). In the particular case of Böhm-Vitense's formalism for energy transport in the superadiabatic stellar layers, one defines a characteristic mixing length being proportional to the pressure height scale $l = \alpha \times \mathrm{Hp}$, in which α is the mixing length parameter. The particular longevity of Böhm-Vitense's formalism goes beyond its adequacy for introducing adjustments to the efficiency of convection. Indeed, it has been shown to be able to reproduce the global properties of solar-type, Population I and red giant branch stars (e.g. Salaris & Cassisi 1996, 2008; Lebreton et al. 1999; Salaris, Cassisi & Weiss 2002). Moreover, the typical mixing length values of these stars ($\alpha \approx 1$) are consistent with the efficiency of the convective energy transport (Cox & Giuli 1968).

In many cases, we scale the unknown parameters taking into account the values resulting from the calibration of the solar values (e.g. Ferraro et al. 2006). In the particular case of the solar mixing length, this is nothing more than the mixing length value of the stellar model that better reproduces a given set of solar observables. Stellar model libraries such as BaSTI (Pietrinferni et al. 2004, 2006) adopt a solar-calibrated mixing length regardless of stellar mass and chemical composition (Pietrinferni et al. 2006). This is not a random choice since, as seen in the case of the BaSTI library, its models are able to reproduce the effective temperature of metal-poor red giant branch stars in globular clusters (Salaris & Cassisi 1996, 2008; Salaris et al. 2002).

However, numerical simulations of the stellar convective layers (Ludwig, Caffau & Kučinskas 2008) and H-R diagram analysis (e.g. Yıldız et al. 2006; Pinheiro et al. 2012) seem to point out against the universality of this parameter. Consequently, in many cases we fail to reproduce the position of a given star in the HRD by assuming such scaling (Lastennet et al. 2003). Yet even when we are able to do so, we might derive incorrect masses and ages (Pinheiro & Fernandes 2010).

Some authors have found hints of a correlation between the mixing length parameter and other stellar parameters such as the stellar mass (e.g. Lebreton, Fernandes & Lejeune 2001) and metallicity (Bonaca et al. 2012), while others foresee an impact of stellar activity on the evolution of low-mass stars which could be mimicked by a different mixing length value (Torres et al. 2006; Chabrier, Gallardo & Baraffe 2007). Therefore, it is important to explore furthermore these results, searching for possible dependence on other global stellar parameters. This paper deals with that issue.

2 STARTING POINT

The stellar models used in this study were computed using the CESAM (Code d'Evolution Stelaire Adaptatif et Modulaire) stellar evolutionary code (Morel 1997). In particular, we used the same physical ingredients adopted in the modelling of subgiant stars of Pinheiro & Fernandes (2010). These include the NACRE compilation of nuclear reaction rates (Angulo et al. 1999), a Grevesse & Noels (1993) mixture of heavy elements, a stellar atmosphere described by an Eddington $T(\tau)$ law, the OPAL equation of state (Rogers, Swenson & Iglesias 1996) and OPAL opacities (Iglesias & Rogers 1996). The latter were complemented, at low temperatures,

⋆ E-mail: fpinheiro@teor.fis.uc.pt

© 2013 The Authors
Published by Oxford University Press on behalf of the Royal Astronomical Society

Downloaded from https://academic.oup.com/mnras/article-abstract/433/4/2893/1747921
by 00500 Universidade de Coimbra user
on 18 July 2018

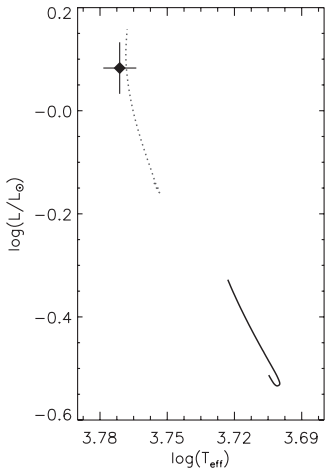

Figure 1. Stellar evolutionary tracks computed taking into account a 1.7 mixing length parameter and both the 0.81 $M_{\odot}$ mass estimate of Cranmer & Saar for 15 Sge (solid line) and our 0.98 $M_{\odot}$ estimate for the same object (dotted line). The diamond corresponds to 15 Sge's position in the H-R diagram.

by Alexander & Ferguson's (1994) opacity tables. Convection is treated using the mixing length theory (Böhm-Vitense 1958), i.e. defining the mixing length $l = \alpha \times \mathrm{Hp}$, where α is the mixing length parameter and Hp is the pressure height scale. No diffusion or overshoot is taken into account in these computations. The initial solar helium and metal abundances used in our computations ($Y_{\odot} = 0.28$ and $Z_{\odot} = 0.017$) were taken from the work of Grevesse & Sauval (1998). Under these conditions, the mixing length value of our model which better reproduces the Sun's effective temperature and luminosity is $\alpha = 1.5$. On the other hand, the initial helium abundance of the remaining stars was estimated taking into account their metal abundance [Fe/X], the solar initial chemical composition and assuming a $\Delta Y/\Delta Z = 2$ helium-to-metal enrichment ratio based on the results of Casagrande et al. (2007): $Y = Y_{\odot} + 2 \times (Z - Z_{\odot})$.

This study also requires a sample of stars for which several of their global properties, namely mass (M), luminosity (L), effective temperature ($T_{\rm eff}$), surface gravity ($\log(g)$), metallicity ([Fe/X]), radius (R), rotation period ($P_{\rm rot}$) and the spatially averaged magnetic flux density ($B \times f$, in which f corresponds to the photospheric filling factor of the magnetic flux tubes). The data resulting from the literature compilation of Cranmer & Saar (2011) provide a good starting point. Due to the heterogeneous nature of this data set, some objects have several measurements of the same observable available, while for other stars the authors do not even provide the uncertainties associated with those measurements. In general terms, these targets present effective temperature uncertainties of the order of 100 K, 0.05 dex uncertainties in stellar luminosity and 0.10 dex in metallicity ([Fe/X]). These values were taken into account in our computations. For some stars, the evolutionary tracks computed using the masses provided by Cranmer & Saar fail by far to reproduce their position in the H-R diagram (as seen in Fig. 1). The 1.46 $M_{\odot}$ mass estimated by Cayrel de Strobel et al. (1989). for the 36 Oph binary (1989) also suggests the unreliability of some of the mass estimates available at Cranmer & Saar's compilation. For this reason, we recomputed the stellar masses using the Padova isochrones (Girardi et al. 2000). These estimates can be found in Table 1. The error estimates shown there are based on the uncertainties associated with the position of these stars in the H-R diagram.

It is important to notice that Cranmer & Saar's sample consists of stars with solar and supersolar metallicities. By adding the targets from Bruntt et al.'s (2010) work, we complement this data set with some metal-poor objects. Moreover, Bruntt et al.'s data set includes a few subgiant and red giant stars. These are valuable since they break away from the well-known relationships found between some of the global stellar parameters of main-sequence stars (Kippenhahn & Weigert 1990), such as the one between the stellar mass and effective temperature. Indeed, Cranmer & Saar's data show a significant degree of correlation [with a false alarm probability (f.a.p.) smaller than 5 per cent] between the stellar mass and other global stellar parameters (see Table 2). Yet due to the small amount of red and subgiant stars available in this sample, there is still some degree of correlation between the stellar mass and the other stellar parameters (see Table 2). For a matter of consistency, Bruntt et al.'s stellar mass estimates were also recomputed using the Padova isochrones (see Table 3). As for the surface gravities, these were estimated taking into account Kjeldsen & Bedding's (1995) relationship between the frequency of maximum power oscillations and the surface gravity. Yet, since Bruntt et al. do not provide an estimate of the errors associated with the frequency of maximum power oscillations, we assumed a typical 0.15 dex uncertainty in the targets' surface gravities.

2.1 Mixing length inference

It is well known that the mixing length has an impact on a stellar model's effective temperature and radius (Kippenhahn & Weigert 1990). This is clearly seen in Fig. 2 (left-hand panel). As a model's mixing length increases, the evolutionary track is shifted towards lower radii/higher effective temperatures. For each evolutionary track, computed assuming a mixing length value, one can determine the effective temperature at which a given luminosity is achieved. Given these two sets of values (effective temperature and mixing length), we defined a function $T_{\rm eff} = g(\alpha)$ converting one set of parameters into the other. This means that the mixing length associated with a given star (α_*) corresponds to the solution of the equation $g(\alpha_*) - T_{\rm eff*} = 0$, where $T_{\rm eff*}$ is the target's effective temperature (as seen in Fig. 2, right-hand panel).

In this particular study, we took into account mixing length values $\alpha = 0.5$, 1.1, 1.3, 1.5, 1.7, 1.9, 2.1 and 5.0. This range includes the typical mixing length values of solar-type stars. Objects whose mixing length fell outside these boundaries were excluded from this analysis. As for the relationship associating each mixing length with an effective temperature, we used a function of the type

$$T_{\rm eff} = A(0) + \frac{A(1)}{\alpha - A(2)}. \quad (1)$$

This function is better suited than linear or parabolic functions since, as α increases, the evolutionary tracks converge towards the case of adiabatic convection.

Note that the mixing length can have a different impact on the evolutionary tracks, depending on the mass of the star and its evolutionary stage. For this reason, each star has to be analysed individually, i.e. for each object we need to find its function $T_{\rm eff} = g(\alpha)$. Moreover, in the case of some subgiant/red giant stars, it is no longer possible to apply the procedure described above. Indeed, as we move away from the main sequence, the linear behaviour described earlier is lost and different evolutionary stages may be able to reproduce the same position in the H-R diagram. Fig. 3 shows two examples of that. Only the study of their non-radial pulsation modes will allow breaking this degeneracy (e.g.

Downloaded from https://academic.oup.com/mnras/article-abstract/433/4/2893/1747921
by 00500 Universidade de Coimbra user
on 18 July 2018

Table 1. Global properties of the targets of Cranmer & Saar (2011) used in this analysis. It also includes mass and mixing length estimates computed taking into account Padova isochrones and the position of these stars in the H-R diagram.

Name	$T_{\rm eff}$	$L/L_\odot$	[Fe/X]	$\log(g)$	$R/R_\odot$	$P_{\rm rot}$	$B \times f$(G)	$M_{\rm Cr}/M_\odot$	$M_{\rm Pad}/M_\odot$	$^{+\Delta M}_{-\Delta M}$	α	$^{+\Delta\alpha}_{-\Delta\alpha}$
59 Vir	6234	1.1000	0.280	4.60	0.897	3.3	345.0	1.17	1.10	$^{+0.09}_{-0.00}$	3.1	$^{+1.4}_{-0.8}$
κ Cet	5771	0.7700	0.056	4.56	0.877	9.4	424.8	1.02	1.01	$^{+0.06}_{-0.05}$	1.8	$^{+0.4}_{-0.4}$
58 Eri	5826	0.8380	−0.013	4.54	0.898	10.8	330.0	1.02	1.00	$^{+0.07}_{-0.06}$	1.8	$^{+0.5}_{-0.4}$
9 Cet	5790	1.1100	0.159	4.40	1.040	7.7	448.0	1.00	1.04	$^{+0.10}_{-0.09}$	1.6	$^{+0.3}_{-0.3}$
Sun	5770	1.0000	0.000	4.44	1.000	25.3	7.7	1.00	1.02	$^{+0.09}_{-0.14}$	1.4	$^{+0.4}_{-0.3}$
HD 28099	5761	1.1000	0.137	4.37	1.050	8.7	510.0	0.94	1.01	$^{+0.13}_{-0.09}$	1.6	$^{+0.4}_{-0.3}$
70 Oph A	5300	0.5300	0.040	4.52	0.860	19.7	216.0	0.89	0.90	$^{+0.08}_{-0.09}$	1.4	$^{+0.4}_{-0.4}$
HD 152391	5495	0.9710	−0.049	4.30	1.090	11.1	306.0	0.86	0.89	$^{+0.06}_{-0.04}$	1.3	$^{+0.2}_{-0.2}$
ξ Boo A	5551	0.5500	−0.122	4.57	0.801	6.2	431.0	0.86	0.90	$^{+0.07}_{-0.10}$	1.7	$^{+0.5}_{-0.5}$
ϵ Eri	5094	0.3450	−0.097	4.60	0.754	11.7	204.9	0.83	0.82	$^{+0.06}_{-0.08}$	1.3	$^{+0.5}_{-0.3}$
15 Sge	5905	1.2100	0.024	4.30	1.050	13.5	180.0	0.81	0.98	$^{+0.17}_{-0.06}$	1.8	$^{+0.4}_{-0.3}$
V833 Tau	4450	0.2090	0.340	4.57	0.770	1.85	1300.0	0.80	0.77	$^{+0.02}_{-0.08}$	0.9	$^{+0.5}_{-0.3}$
LQ Hya	5070	0.2700	0.330	4.68	0.673	1.6	2450.0	0.80	0.83	$^{+0.05}_{-0.03}$	2.9	$^{+1.7}_{-1.1}$
HD 17925	5225	0.5800	0.067	4.40	0.930	6.6	525.0	0.79	0.85	$^{+0.09}_{-0.04}$	1.3	$^{+0.4}_{-0.3}$
DE Boo	5231	0.5120	0.108	4.45	0.871	9.0	102.0	0.78	0.85	$^{+0.12}_{-0.03}$	1.5	$^{+0.5}_{-0.4}$
HD 4628	5004	0.2730	−0.270	4.64	0.690	38.5	192.0	0.77	0.77	$^{+0.04}_{-0.08}$	1.2	$^{+0.3}_{-0.3}$
HD 115404	4814	0.3030	−0.193	4.53	0.791	18.8	420.0	0.77	0.74	$^{+0.08}_{-0.04}$	0.9	$^{+0.5}_{-0.2}$
61 Cyg A	4425	0.1530	−0.193	4.63	0.665	35.4	288.0	0.69	0.66	$^{+0.06}_{-0.04}$	0.9	$^{+1.0}_{-0.3}$
EQ Vir	4179	0.1600	−0.075	4.50	0.762	3.98	1687.5	0.67	0.68	$^{+0.02}_{-0.05}$	0.5	$^{+0.3}_{-0.1}$
χ^1 Ori	5955	1.0500	−0.039	4.30	0.962	5.2	600.0	0.67	0.98	$^{+0.14}_{-0.07}$	1.9	$^{+0.6}_{-0.4}$
OU Gem	4959	0.4570	−0.170	4.30	0.915	7.4	1200.0	0.61	0.79	$^{+0.05}_{-0.04}$	0.8	$^{+0.3}_{-0.2}$
36 Oph A	5135	0.2990	−0.206	4.54	0.690	20.3	195.0	0.60	0.76	$^{+0.08}_{-0.04}$	2.0	$^{+2.9}_{-0.8}$

Table 2. Linear correlation coefficients between stellar mass and other stellar parameters (r) and f.a.p. associated.

	Cranmer & Saar		Bruntt et al.		All	
Comparison	r	f.a.p. (per cent)	r	f.a.p. (per cent)	r	f.a.p. (per cent)
$M_{\rm Pad}$ versus $\log(T_{\rm eff})$	0.94	<0.1	0.31	20.5	0.61	<0.1
$M_{\rm Pad}$ versus $\log(L/L_\odot)$	0.93	<0.1	0.74	<0.1	0.85	<0.1
$M_{\rm Pad}$ versus $\log(R)$:	0.73	<0.1	0.61	0.8	0.74	<0.1
$M_{\rm Pad}$ versus [Fe/X]:	0.46	3.0	0.49	3.9	0.31	5.2
$M_{\rm Pad}$ versus $\overline{B \times f}$	−0.32	14.1				

Pinheiro & Fernandes 2010). Nonetheless, it is still possible to identify the mixing length values that allow us to reproduce the positions of these particular targets in the H-R diagram (as seen in Fig. 3).

Tables 1 and 3 present the results from applying the procedures mentioned above to our data. Once more, the error estimates are based on the uncertainties associated with these objects' position in the H-R diagram. Note that some targets have two possible solutions. Yet one of these solutions tends to be well below the lowest mixing length value used in our computations ($\alpha = 0.5$), which is a value well below those normally seen in these type of stars. For that reason, in those cases we only took into account the other solution.

2.2 Mass uncertainty

The difference between the masses inferred using the Padova isochrones and the ones given by Cranmer & Saar poses the question of the mass uncertainty's impact on the mixing length determination. Prior to any calculation, one can already expect that, for stars located on the main sequence, an assumption of a mass higher than the real value will result in an α estimation below the real value.

For those cases in which both mass estimates (those from the Padova models and those from Cranmer & Saar) were able to reproduce the targets' luminosity, we found a maximum difference of α of 0.16, corresponding to $\mathrm{d}\alpha/\mathrm{d}M \approx -5.4$. Yet, for most objects with a typical solar mixing length value, the $\mathrm{d}\alpha/\mathrm{d}M$ ratio tends to be about −3. Taking into account that mass uncertainties tend to be of the order of 0.1–0.2 $M_\odot$, mixing length uncertainties around 0.3 and 0.6 are obtained, which are clearly enough to identify subsolar mixing length values.

2.3 Metallicity uncertainty

In the same way as it occurs in the determination of stellar masses, different groups can obtain different stellar metallicity estimates. For instance, the metallicity [Fe/H] equal to +0.12 reported by Bruntt et al. (2010) for 70 Oph A is slightly higher than the +0.04

Downloaded from https://academic.oup.com/mnras/article-abstract/433/4/2893/1747921
by 00500 Universidade de Coimbra user
on 18 July 2018

Table 3. Global properties of the targets of Bruntt et al. (2010) used in our analysis. This includes a comparison between the masses reported by Bruntt et al. and those computed using the Padova isochrones. The uncertainties on each target's mass and mixing length parameter are based on the uncertainty of their position in the H-R diagram.

Name	$T_{\rm eff}$	$L/L_\odot$	[Fe/X]	$\log(g)$	$R/R_\odot$	$M_{\rm Br}/M_\odot$	$M_{\rm Pad}/M_\odot$	$^{+\Delta M}_{-\Delta M}$	α	$^{+\Delta\alpha}_{-\Delta\alpha}$	$\alpha_{\rm alternative}$	
βHyi	5790	3.57	−0.10	3.95	1.89	1.08	1.13	$^{+0.04}_{-0.03}$	1.1	$^{+0.4}_{-0.1}$		
τCet	5290	0.50	−0.48	4.59	0.85	0.79	0.78	$^{+0.03}_{-0.03}$	1.0	$^{+0.3}_{-0.1}$		
ιHor	6080	1.64	0.15	4.40	1.16	1.23	1.20	$^{+0.02}_{-0.10}$	1.6	$^{+0.5}_{-0.2}$		
δEri	5015	3.26	0.15	3.77	2.41	1.33	1.26	$^{+0.03}_{-0.14}$	1.3	$^{+0.1}_{-0.1}$	≤0.1	
αMen	5570	0.83	0.15	4.77[a]	0.99	–	1.00	$^{+0.05}_{-0.11}$	1.4	$^{+0.4}_{-0.1}$		
Proc A	6485	7.17	0.01	3.98	2.13	1.46	1.50	$^{+0.03}_{-0.15}$	1.7	$^{+0.5}_{-0.3}$		
171 Pup	5710	1.46	−0.86	4.26	1.24	0.99	0.82	$^{+0.01}_{-0.01}$	0.7	$^{+0.2}_{-0.1}$		
ξHya	5045	59.38	0.21	2.88	10.14	2.89	2.85	$^{+0.00}_{-0.15}$	1.9	$^{+0.3}_{-0.1}$	1.0	$^{+0.3}_{-0.3}$
βVir	6050	3.40	0.12	4.11	1.69	1.42	1.29	$^{+0.04}_{-0.13}$	1.0	$^{+0.6}_{-0.4}$		
ηBoo	6030	8.66	0.24	3.84	2.66	1.77	1.59	$^{+0.05}_{-0.11}$	2.4	$^{+0.5}_{-0.2}$	≤0.1	
αCen A	5745	1.51	0.22	4.33	1.24	1.11	1.06	$^{+0.05}_{-0.07}$	1.5	$^{+0.3}_{-0.1}$		
αCen B	5145	0.51	0.30	4.54	0.91	0.93	0.86	$^{+0.10}_{-0.02}$	1.4	$^{+0.5}_{-0.1}$		
γSer	6115	3.02	−0.26	4.17	1.55	1.30	1.15	$^{+0.04}_{-0.16}$	0.9	$^{+0.5}_{-0.4}$		
μAra	5665	1.78	0.32	4.25	1.39	1.21	1.05	$^{+0.06}_{-0.04}$	1.6	$^{+0.3}_{-0.1}$		
70 Oph A	5300	0.59	0.12	4.59	0.91	0.89	0.87	$^{+0.12}_{-0.03}$	1.4	$^{+0.5}_{-0.1}$		
ηSer	4850	18.32	−0.11	3.03	6.10	1.45	1.44	$^{+0.41}_{-0.27}$	1.7	$^{+0.2}_{-0.1}$		
βAql	5030	6.23	−0.21	3.54	3.30	1.26	1.28	$^{+0.14}_{-0.22}$	1.6	$^{+0.3}_{-0.1}$	0.9	$^{+0.2}_{-0.2}$
δPav	5550	1.22	0.38	4.31	1.20	1.07	1.00	$^{+0.03}_{-0.07}$	1.5	$^{+0.3}_{-0.0}$		
γPav	5990	1.52	−0.74	4.38	1.15	1.21	0.84	$^{+0.02}_{-0.03}$	1.2	$^{+0.4}_{-0.1}$		
τPsA	6235	2.82	0.01	4.26	1.45	1.34	1.22	$^{+0.06}_{-0.04}$	1.3	$^{+0.5}_{-0.1}$		
νInd	5140	6.28	−1.63	3.43	3.18	1.00	0.82	$^{+0.02}_{-0.01}$	1.1	$^{+0.2}_{-0.1}$		

[a]Computed using $M_{\rm Pad}$ and $R/R_\odot$.

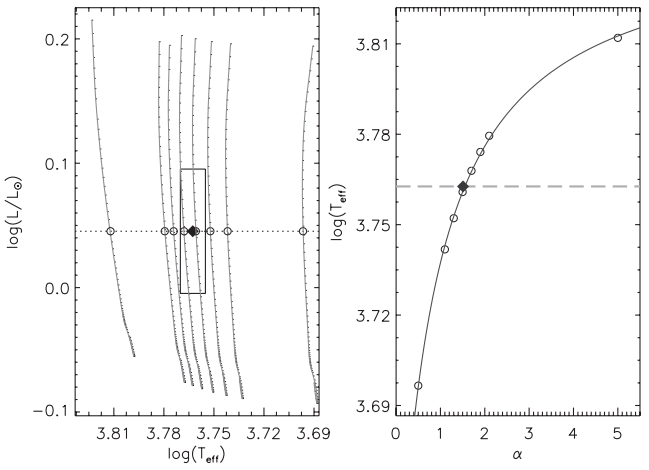

Figure 2. Left: evolutionary tracks of 1.043 $M_\odot$ stars with mixing lengths between 5.0 (leftmost track) and 0.5 (rightmost track). The diamond corresponds to 9 Cet's position in the H-R diagram, the box corresponds to uncertainty associated with its position and the circles correspond to the model's 9 Cet's luminosity (dotted line) for a given mixing length value. Right: effective temperature of the best model solutions as a function of their mixing length parameter. The dashed line corresponds to 9 Cet's effective temperature.

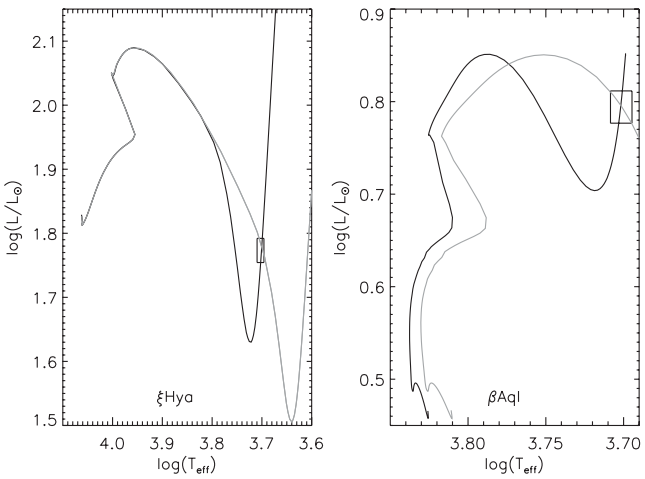

Figure 3. Evolutionary tracks reproducing the position of ξHya (left-hand panel) and βAql (right-hand panel) in the H-R diagram. The boxes correspond to uncertainties associated with the position of these stars in the H-R diagram. The evolutionary tracks were computed assuming $\alpha = 1.9$ (black lines) and 0.95 (grey lines) for ξHya and $\alpha = 1.63$ (black lines) and 0.85 (grey lines) for βAql.

metallicity of Cranmer & Saar (2011). This difference is of the same order of magnitude as the metallicity uncertainties reported by Bruntt et al. (2010). In the particular case of 70 Oph A, we found a 0.13 difference in the mixing length estimate (see Fig. 4). Such a result suggests that, in comparison to other parameters, small metallicity uncertainties may not have a substantial impact on the mixing length determination.

3 DEPENDENCE ON GLOBAL PARAMETERS

The mixing length parameters inferred using the methodology discussed above (see Tables 1 and 3) clearly point out against the

Downloaded from https://academic.oup.com/mnras/article-abstract/433/4/2893/1747921
by 00500 Universidade de Coimbra user
on 18 July 2018

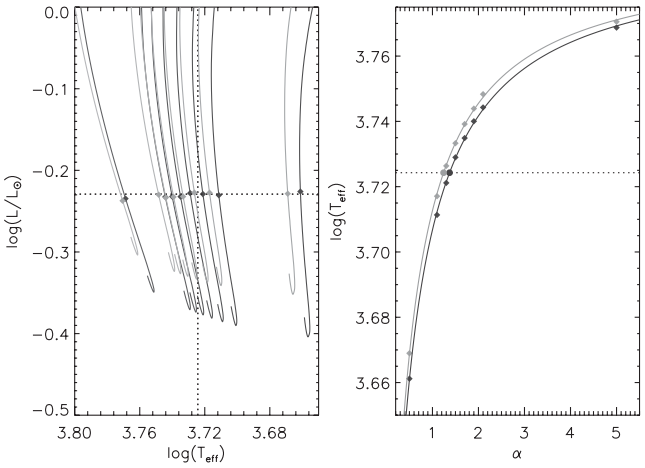

Figure 4. Left: evolutionary tracks for 0.89 $M_{\odot}$ models with α comprised between 0.5 and 5.0 and a metallicity [Fe/H] equal to +0.12 (black lines) and +0.04 (grey lines). The diamonds correspond to the models that better reproduce 70 Oph A's luminosity (denoted by the dotted lines). Right: interpolation of 70 Oph A's mixing length, assuming a metallicity [Fe/H] equal to +0.12 (black circle) and +0.04 (grey circle).

universality of the mixing length. This motivated the search for possible correlations between the mixing length parameter and some global stellar parameters. This was carried out using the models for which the inferred mixing length falls within the range of the models used here (i.e. those with $0.5 \leq \alpha \leq 5.0$), which correspond to the typical mixing length values of solar-type stars. Likewise, the objects with two possible mixing length values within this range were also excluded from this study. The results from our analysis are shown in Table 4.

Fig. 5 hints at a correlation between the target's mixing length and both their mass and effective temperature. In both cases, the linear correlation coefficient corresponds to a f.a.p. below 1 per cent. Taking into account the high degree of correlation between our data's mass and their effective temperature, it is still difficult to identify which one of these two parameters is having a key role in the observed correlations. Yet, in the case of Bruntt et al. subsample, which includes three red giant stars, we observe a significant lower degree of correlation between the effective temperature and the mixing length. The same does not occur for the stellar mass. This hints that the stellar mass is the parameter having a key role in the observed correlations. It is interesting to note that just like Bonaca et al. (2012) data, Bruntt et al. subsample does not display a significant correlation between the mixing length and effective temperature. Yet both samples do not include very cold stars ($T_{\rm eff} \leq$ 5000 K). Therefore, one cannot exclude the possibility of being the case of a sampling bias.

The combined Cranmer & Bruntt data show a significant degree of correlation between the mixing length and stellar metal abundance. In order to remove the possible mixing length dependence on the effective temperature, we subtracted from it a function of the type $\alpha = 4.83 \times T_{\rm eff} - 16.59$, which results from a linear fit to the data (dotted line in Fig. 5). Even so, we still find a significant degree of linear correlation ($r = 0.41$ and f.a.p = 0.9 per cent) between the metal abundance and the residuals of the mixing length. Such a conclusion is similar to the results of Bonaca et al. (2012). On the other hand, after removing a function $\alpha = 0.60{+}0.87{\times}M$ (dashed line in Fig. 5) from our mixing length estimates, we find a degree of correlation between the metal abundance and the residuals close to a level in which we can no longer ignore the null hypothesis ($r = 0.32$ and f.a.p. = 4.2).

On the other hand, despite some degree of correlation between our combined data's mass and their surface gravity, stellar luminosity and radius, no significant degree of linear correlation was found between these parameters and the mixing length. One might have expected some degree of correlation between the mixing length and the stellar luminosity (which occurs for the Cranmer data alone), attending to the mass luminosity relationship for main-sequence stars and the high mass–mixing length correlation seen here.

In its own turn, no significant correlations were found between the mixing length and either surface gravity or luminosity. Likewise, no significant degree of linear correlation was found between the mixing length and several indicators of stellar activity such as the rotation period, the ratio between stellar radius and the rotation period (a proxy for the rotation velocity) and the mean of the spatially averaged magnetic flux density measurements available ($\overline{B \times f}$). The lack of stars with stronger magnetic field densities ($B \times f \geq$ 1000 G), particularly amongst the more massive stars, may constitute a bias affecting the conclusions made regarding any possible correlation between the mixing length parameter and the targets' magnetic fields.

However, these results do not take into account the uncertainties associated with each parameter. Indeed, in our Monte Carlo simulations we were only able to find significant correlation coefficients in less than half of the realizations. This result is furthermore stressed by the fact that our mixing length estimates are only based on the uncertainties of each target's position in the H-R diagram. That means that despite having found strong indications of a correlation between the mixing length and some global stellar parameters, we cannot be conclusive about them. Our Monte Carlo simulations seem to indicate that this can only be achieved with mixing length

Table 4. Linear correlation coefficient (r) between the mixing length and other stellar parameters, and its associated f.a.p.

	Cranmer & Saar		Bruntt et al.		All	
Comparison	r	f.a.p. (per cent)	r	f.a.p. (per cent)	r	f.a.p (per cent)
$M_{\rm Pad}$ versus α	0.60	0.3	0.65	0.4	0.36	2.3
$T_{\rm eff}$ versus α	0.66	0.1	0.08	75.4	0.40	1.0
log$G$ versus α	0.21	35.7	−0.22	39.0	0.05	77.3
log$L$ versus α	0.45	3.7	0.37	13.3	0.16	32.9
log$R$ versus α	0.06	77.8	0.32	19.2	0.01	94.2
Fe/X versus α	0.50	1.7	0.53	2.4	0.41	0.8
$P_{\rm rot}$ versus α	−0.30	17.2				
$R/P_{\rm rot}$ versus α	0.36	9.9				
$\overline{B \times f}$ versus α	0.06	80.6				

Downloaded from https://academic.oup.com/mnras/article-abstract/433/4/2893/1747921
by 00500 Universidade de Coimbra user
on 18 July 2018

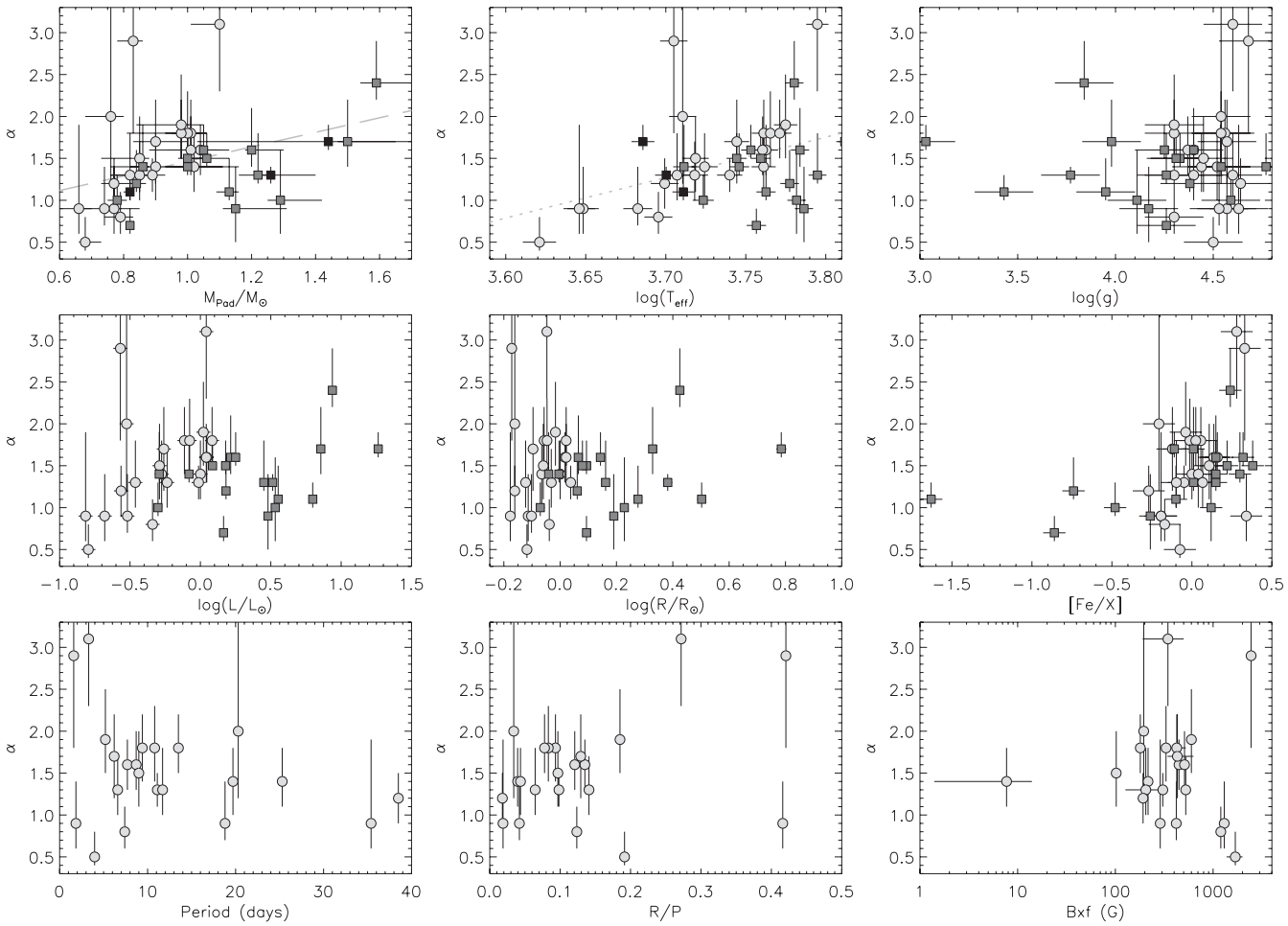

Figure 5. Comparison between our targets' mixing length parameter and several global stellar parameters, namely mass, effective temperature, surface gravity, luminosity, stellar radius, metal abundance, stellar radius–rotation period ratio (proxy of the rotation velocity) and magnetic field strength. The diamonds and squares correspond, respectively, to the targets from Cranmer & Saar (2011) and Bruntt et al.'s (2010) data. The black squares correspond to red giant stars. The dashed and dotted grey lines correspond to the best linear fits to the data used in this analysis. The circles in the lower-right panel correspond to the average of the spatially averaged magnetic flux density measurements reported by Cranmer & Saar ($\overline{B \times f}$), while the horizontal bars correspond to the individual measurements.

uncertainties of the order of 0.1. In complement/alternative to that we must substantially increase the size of our sample.

4 CONCLUSIONS AND DISCUSSION

In this work, we have observed indications of a strong correlation between the mass and mixing length parameter of solar-type stars. Such a result is similar to the one obtained by Lebreton et al. (2001). Yet, unlike in the study of stars of the Hyades cluster, in the present case we are not limited to objects of a similar metal abundance. This conclusion clearly goes against the still common practice of assuming solar value of mixing length when modelling other solar-type stars.

Nonetheless, it is interesting to recall that the solar-calibrated models are still able to make a good job reproducing the properties of several field stars including star clusters and eclipsing binaries (e.g. Salaris & Cassisi 1996, 2008; Salaris et al. 2002).

Additionally, according to the numerical simulations of Ludwig et al. (2008) and Trampedach & Stein (2011), the mixing length should present an anticorrelation with respect to the effective temperature. This is exactly the opposite of what is being seen here. Yet, Ludwig's result was obtained using a constant metallicity value. Moreover, both the Lebreton et al. (2001) and Yıldız et al. (2006) studies of the Hyades cluster (2001), which also use objects with a similar metal abundance, point out in the same direction as our result.

The correlation between the mixing length parameter and both the stellar mass and effective temperature hinted here could be seen under the fact that these parameters have an impact on the size of the superadiabatic layer. Yet one must not discard the fact that in main-sequence stars, there is a strong correlation between the stellar mass and effective temperature. The inclusion of additional red and subgiant stars in future works will be valuable since they depart from the relationship mentioned above. Yet, in some particular cases, one may find more than one possible solution for their mixing length parameter. Nevertheless, the study of non-radial pulsation modes may provide a valuable tool for breaking this degeneracy of solutions (e.g. Pinheiro & Fernandes 2010).

The determination of which parameter, mass or effective temperature, is having a greater impact on the mixing length parameter has important implications for stellar modelling. For instance, if the mixing length depends on the effective temperature, then the stellar evolution codes should take into account mixing length

Downloaded from https://academic.oup.com/mnras/article-abstract/433/4/2893/1747921
by 00500 Universidade de Coimbra user
on 18 July 2018

variations as the star evolves along the subgiant branch. Such concern is irrelevant in the case of a mass dependence.

On the other hand, we have found a significant degree of correlation between our target's mixing length parameter and their effective temperature. Such a correlation was not found by Bonaca et al. (2012) nor in our analysis of Bruntt et al.'s (2010) subsample. Yet neither the analysis of Bonaca et al. (2012) nor Bruntt et al.'s (2010) study take into account low-mass stars ($M \leq 0.8\,\mathrm{M}_{\odot}$), which is the same as saying colder stars ($T_{\mathrm{eff}} \leq 5000\,\mathrm{K}$). A correlation between some of the global stellar parameters, in addition to a possible sampling bias, may be the reason behind this discrepancy of results. This clearly stresses the importance of improving the completeness of the data.

Finally, contrary to Torres et al.'s (2006) expectation, we have found no strong indications of a possible correlation between the mixing length parameter and indicators of stellar activity such as magnetic field strength or the rotation velocity. Despite that, some data points in Fig. 5 (lower-right panel) seem to suggest such a correlation. Moreover, the lack of massive stars with strong spatially averaged magnetic flux densities (above kG) in our sample makes it advisable to further study this issue. For this reason, we intend to explore furthermore this subject.

The uncertainties on the mixing length determination have greatly affected the statistical significance of the results presented here. Asteroseismology can be used to infer the mixing length and other global parameters with greater accuracy (e.g. Mathur et al. 2012). In the future we plan to enlarge our sample using such data from the *Kepler* and *COROT* asteroseismic missions. Furthermore, additional targets will improve the completeness of the sample and the statistical significance of correlation coefficients.

ACKNOWLEDGEMENTS

This work was supported by Fundação para a Ciência e a Tecnologia (FCT). FJGP also acknowledges grant /SFRH/BPD/37491/2007 from FCT, co-financed by the European Social Fund. The authors would also like to thank the anonymous referee for his useful remarks.

REFERENCES

Alexander D. R., Ferguson J. W., 1994, ApJ, 437, 879
Angulo C. et al., 1999, Nucl. Phys. A, 656, 3
Böhm-Vitense E., 1958, Z. Astrophys., 46, 108
Bonaca A. et al., 2012, ApJ, 755, L12
Bruntt H. et al., 2010, MNRAS, 405, 1907
Casagrande L., Flynn C., Portinari L., Girardi L., Jimenez R., 2007, MNRAS, 382, 1516
Cassisi S., 2005, preprint (arXiv:astro-ph/0506161)
Cayrel de Strobel G., Lebreton Y., Perrin M.-N., Cayrel R., 1989, A&A, 225, 369
Chabrier G., Gallardo J., Baraffe I., 2007, A&A, 472, L17
Cox J. P., Giuli R. T., 1968, Principles of Stellar Structure: Physical Principles. Gordon and Breach, New York
Cranmer S. R., Saar S. H., 2011, ApJ, 741, 54
Ferraro F. R., Valenti E., Straniero O., Origlia L., 2006, ApJ, 642, 225
Girardi L., Bressan A., Bertelli G., Chiosi C., 2000, A&AS, 141, 371
Grevesse N., Noels A., 1993, Origin and Evolution of the Elements. Cambridge Univ. Press, Cambridge, p. 15
Grevesse N., Sauval A. J., 1998, Space Sci. Rev., 85, 161
Iglesias C. A., Rogers F. J., 1996, ApJ, 464, 943
Kippenhahn R., Weigert A., 1990, Stellar Structure and Evolution. Vol. XVI, Springer-Verlag, Berlin, p. 468
Kjeldsen H., Bedding T. R., 1995, A&A, 293, 87
Lastennet E., Fernandes J., Valls-Gabaud D., Oblak E., 2003, A&A, 409, 611
Lebreton Y., Perrin M.-N., Cayrel R., Baglin A., Fernandes J., 1999, A&A, 350, 587
Lebreton Y., Fernandes J., Lejeune T., 2001, A&A, 374, 540
Ludwig H.-G., Caffau E., Kučinskas A., 2008, in Deng L., Chan K. L., eds, IAU Symp. 252, Radiation-hydrodynamics Simulations of Surface Convection in Low-mass Stars: Connections to Stellar Structure and Asteroseismology. Cambridge Univ. Press, Cambridge, p. 75
Mathur S. et al., 2012, ApJ, 749, 152
Morel P., 1997, A&AS, 124, 597
Pietrinferni A., Cassisi S., Salaris M., Castelli F., 2004, ApJ, 612, 168
Pietrinferni A., Cassisi S., Salaris M., Castelli F., 2006, ApJ, 642, 797
Pinheiro F. J. G., Fernandes J. M., 2010, Ap&SS, 328, 73
Pinheiro F. J. G., Simas T., Fernandes J., Ribeiro R., 2012, New Astron., 17, 629
Rogers F. J., Swenson F. J., Iglesias C. A., 1996, ApJ, 456, 902
Salaris M., Cassisi S., 1996, A&A, 305, 858
Salaris M., Cassisi S., 2008, A&A, 487, 1075
Salaris M., Cassisi S., Weiss A., 2002, PASP, 114, 375
Torres G., Lacy C. H., Marschall L. A., Sheets H. A., Mader J. A., 2006, ApJ, 640, 1018
Trampedach R., Stein R. F., 2011, ApJ, 731, 78
Yıldız M., Yakut K., Bakış H., Noels A., 2006, MNRAS, 368, 1941

This paper has been typeset from a TEX/LATEX file prepared by the author.

Downloaded from https://academic.oup.com/mnras/article-abstract/433/4/2893/1747921
by 00500 Universidade de Coimbra user
on 18 July 2018